



## Article

# The Effect of Paracrine Factors Released by Irradiated Peripheral Blood Mononuclear Cells on Neutrophil Extracellular Trap Formation

Katharina Klas<sup>1,2</sup>, Anna S. Ondracek<sup>3</sup> , Thomas M. Hofbauer<sup>3</sup> , Andreas Mangold<sup>3</sup>, Karin Pfisterer<sup>4</sup> , Maria Laggner<sup>1,2</sup>, Dragan Copic<sup>1,2</sup> , Martin Direder<sup>1,2</sup>, Daniel Bormann<sup>1,2</sup>, Hendrik Jan Ankersmit<sup>1,2,\*</sup>,† and Michael Mildner<sup>4,\*</sup>

<sup>1</sup> Laboratory for Cardiac and Thoracic Diagnosis, Regeneration and Applied Immunology, Department of Thoracic Surgery, Medical University of Vienna, 1090 Vienna, Austria

<sup>2</sup> Aposcience AG, 1200 Vienna, Austria

<sup>3</sup> Division of Cardiology, Department of Internal Medicine II, Vienna General Hospital, Medical University of Vienna, 1090 Vienna, Austria

<sup>4</sup> Department of Dermatology, Medical University of Vienna, 1090 Vienna, Austria

\* Correspondence: hendrik.ankersmit@meduniwien.ac.at (H.J.A.); michael.mildner@meduniwien.ac.at (M.M.)

† These authors contributed equally to this work.



**Citation:** Klas, K.; Ondracek, A.S.; Hofbauer, T.M.; Mangold, A.; Pfisterer, K.; Laggner, M.; Copic, D.; Direder, M.; Bormann, D.; Ankersmit, H.J.; et al. The Effect of Paracrine Factors Released by Irradiated Peripheral Blood Mononuclear Cells on Neutrophil Extracellular Trap Formation. *Antioxidants* **2022**, *11*, 1559. <https://doi.org/10.3390/antiox11081559>

Academic Editors: Mercedes Camacho Pérez de Madrid and Josep Julve

Received: 29 July 2022

Accepted: 10 August 2022

Published: 11 August 2022

**Publisher's Note:** MDPI stays neutral with regard to jurisdictional claims in published maps and institutional affiliations.



**Copyright:** © 2022 by the authors. Licensee MDPI, Basel, Switzerland. This article is an open access article distributed under the terms and conditions of the Creative Commons Attribution (CC BY) license (<https://creativecommons.org/licenses/by/4.0/>).

**Abstract:** Neutrophil extracellular trap (NET)-formation represents an important defence mechanism for the rapid clearance of infections. However, exaggerated NET formation has been shown to negatively affect tissue-regeneration after injury. As our previous studies revealed the strong tissue-protective and regenerative properties of the secretome of stressed peripheral blood mononuclear cells (PBMsec), we here investigated the influence of PBMsec on the formation of NETs. The effect of PBMsec on NET formation was assessed *ex vivo* in ionomycin stimulated neutrophils derived from healthy donors using flow cytometry, image stream analysis, and quantification of released extracellular DNA. The effect of PBMsec on molecular mechanisms involved in NET formation, including Ca-flux, protein kinase C activity, reactive oxygen species production, and protein arginine deiminase 4 activity, were analysed. Our results showed that PBMsec significantly inhibited NET formation. Investigation of the different biological substance classes found in PBMsec revealed only a partial reduction in NET formation, suggesting a synergistic effect. Mechanistically, PBMsec treatment did not interfere with calcium signalling and PKC-activation, but exerted antioxidant activity, as evidenced by reduced levels of reactive oxygen species and upregulation of heme oxygenase 1 and hypoxia inducible-factor 1 in PBMsec-treated neutrophils. In addition, PBMsec strongly inhibited the activation of protein arginine deiminase 4 (PAD4), ultimately leading to the inhibition of NET formation. As therapeutics antagonizing excessive NET formation are not currently available, our study provides a promising novel treatment option for a variety of conditions resulting from exaggerated NET formation.

**Keywords:** neutrophil; neutrophil extracellular traps (NETs); PAD4; ROS; secretome; peripheral blood mononuclear cell secretome

## 1. Introduction

Neutrophil granulocytes represent the main population of circulating leukocytes in the blood [1]. They exert a plethora of functions critical for maintaining immune homeostasis, and their contribution to immune regulatory mechanisms is of vital importance during infectious conditions [2]. Being amongst the first cell populations to be recruited to a site of infection, they use a broad machinery of defence mechanisms, including the production of reactive oxygen species (ROS), excretion of cytotoxic granules, phagocytosis of pathogens, and the formation of neutrophil extracellular traps (NETs), to fight invading

pathogens [3]. In addition to these functions, NET formation represents another potent defence mechanism for the elimination of pathogens [4]. Neutrophils are equipped with a vast array of surface receptors, including Toll-like and NOD-like receptors, G-protein coupled receptors, cytokine receptors, as well as Fc and complement receptors, rendering them highly responsive to a multitude of stimuli [5]. Some of these stimuli, such as ROS or bacterial toxins, are potent inducers of NETs and operate independently of the classical neutrophil activation pathways via surface receptors [6–8]. After induction of NET formation, intracellular  $\text{Ca}^{2+}$  levels increase due to influx and its release from the endoplasmic reticulum, promoting protein kinase C (PKC) activation and phosphorylation of  $\text{Gp91}^{\text{phox}}$  [9]. Activation of PKC, in turn, leads to the assembly of functional NADPH oxidase, which generates reactive oxygen species (ROS) [10]. Furthermore, increased  $\text{Ca}^{2+}$  levels activate protein arginase deiminase 4 (PAD4) [11], which promotes chromatin decondensation by converting arginine residues of core histones H3 and H4 into citrulline [8]. In addition, ROS also lead to the gradual disassembly of the nuclear membrane, followed by the dispersion of chromatin throughout the cytoplasm, where it is decorated with granular and cytoplasmic contents [12]. Ultimately, chromatin, DNA, granular, and cytoplasmic contents are released into the extracellular space as NETs [6,13].

Neutrophil functions, specifically the extrusion of NETs, are considered beneficial during infection [14]. However, dysregulated or extensive NET formation may result in undesirable tissue damage [15,16] and is linked to many inflammatory disorders, including sepsis, asthma, lupus, rheumatologic diseases, as well as diabetes [17]. Additionally, neutrophils receive increasing interest in cancer research as potential drivers of metastasis [18]. Furthermore, NETs are discussed as potential inducers of endothelial tissue damage, leading to various forms of vasculitis [19]. The accumulation of neutrophils, as well as the entailing activation and NET formation, at the culprit site lesion during acute coronary syndrome or acute myocardial infarction, is associated with poor disease prognosis and an increased long-term mortality rate [20–22]. In addition to systemic disorders, excessive NET formation is also associated with locally impaired or prolonged tissue regeneration, due to increased neutrophil-derived ROS in the microenvironment of the injury [16,23–26].

Recent advances in cell-derived, yet cell-free medicinal products have increasingly gained attention in regenerative medicine [27,28]. Although initial research on cell-free therapeutic agents focused on secretomes derived from stem cells, we could demonstrate that the secretome of peripheral blood mononuclear cells (PBMC) exhibits comparable regenerative effects [29–35]. The potency of the PBMC-derived secretome (PBMCsec) was further increased by exposing PBMCs to 60 Gy  $\gamma$ -irradiation, which induces apoptosis and necroptosis, resulting in the release of a plethora of pro-regenerative paracrine factors [29]. Lichtenauer et al. showed strong regenerative potential of PBMCsec in rodent and porcine models of acute myocardial infarction [35]. These pioneering findings laid the foundation for further studies, which identified a broad spectrum of therapeutic implications for PBMCsec in a vast variety of pathologic conditions, including chronic heart failure after myocardial infarction [36], cerebral ischemia [35], burn injury [35], diabetic wound healing [30], and acute spinal cord injury [35]. Furthermore, strong anti-inflammatory properties of PBMCsec have been demonstrated in the context of myocarditis [35], as well as inflammatory skin conditions [34]. The observed tissue-regenerative effect of PBMCsec is based on a complex interplay of various biologically active agents produced and released by stressed PBMCs [30,32,35]. The broad action spectrum of PBMCsec has been intensively investigated and revealed promising treatment opportunities, where anti-inflammatory [37,38], anti-microbial [33], tissue-regenerative [32], pro-angiogenic [29,30], and vasodilatory [35] properties are important.

Although PBMCsec possesses compelling immunomodulatory effects [35], potential anti-inflammatory and stabilizing effects on (activated) neutrophils have not been investigated so far. Hence, we sought to investigate the effect of PBMCsec on NET formation.

## 2. Materials and Methods

### 2.1. Ethics Statement

This study was conducted in accordance with the Declaration of Helsinki and applicable local regulations. Use of human neutrophils was approved by the institutional ethical review board of the Medical University of Vienna (Vienna, Austria) (protocol code 1539/2017). Written informed consent was obtained from all donors.

### 2.2. Generation of PBMCsec

PBMCsec was produced in compliance with good manufacturing practice by the Austrian Red Cross, Blood Transfusion Service for Upper Austria (Linz, Austria) as previously described [30,34]. Briefly, the PBMCs were enriched using Ficoll-Paque PLUS (GE Healthcare, Chicago IL, USA) density gradient centrifugation. Cell suspensions were adjusted to  $2.5 \times 10^7$  cells/mL and exposed to 60 Gy  $\gamma$ -irradiation (IBL 437, Isotopen Diagnostik CIS GmbH, Dreieich, Germany). Subsequently, cells were cultured in phenol red-free CellGenix GMP DC medium (CellGenix, Freiburg, Germany) for 24 h. Cells, as well as cellular debris, were removed by centrifugation. The conditioned supernatants containing the secretome were filtered through 0.22  $\mu$ m filters followed by viral clearance using Theraflex methylene blue technology (MacoPharma, Mouvoux, France). The secretomes were lyophilized and sterilized by high-dose  $\gamma$ -irradiation (25,000 Gy, Gammatron 1500, Mediscan, Seibersdorf, Austria). CellGenix GMP DC medium without cells was used as vehicle control. The GMP batches A000918399131, A00918399136, and A000918399132 were used in this study. The stock concentration of one vial lyophilized secretome equals to 25 units/mL.

### 2.3. Fractionating PBMCsec

The lipid fraction was purified according to Folch et al. (PMID: 13428781) with minor modifications. Briefly, one part reconstituted PBMCsec was mixed with 9 parts 2:1 (*vol/vol*) chloroform–methanol and, subsequently, excessively vortexed. Then, 0.7 M of formic acid was used to acidify the emulsion (a one-fourth volume of the chloroform–methanol mix) and homogenized by thorough shaking. Phase separation was obtained by leaving the samples on ice for 30 min. The lower, organic phase was further applied to rotary vacuum evaporation (475 mbar, 100 rpm, 60 °C water bath temperature) in order to eliminate solvents. The protein fraction was isolated by combining four times the volume of ice-cold acetone (VWR Chemicals, PA, USA) to one volume of reconstituted PBMCsec, followed by thorough vortexing and incubation at  $-20$  °C for 60 min, to obtain a protein precipitate. After centrifuging the sample at  $18,000 \times g$  for 10 min, ice-cold acetone was added to the protein pellet, briefly vortexed and centrifuged at  $18,000 \times g$  for 10 min. Acetone was discarded and remaining acetone was allowed to evaporate at room temperature. Finally, the protein pellet was resuspended in 0.9% NaCl in the initially used volume. DNA was isolated by adding equal amounts of isopropanol (Merck Millipore, MA, USA) as PBMCsec and 1/10 volume of 7.5 M sodium acetate (Merck Millipore) and incubated at  $-20$  °C for 1 h. After centrifugation for 5 min at  $18,000 \times g$  the DNA pellet was washed twice with 1 mL 70% Ethanol (Merck Millipore) followed centrifugation at  $18,000 \times g$  for 5 min. The DNA pellet was allowed to dry for 10 min at room temperature prior to resuspension in double distilled, nuclease-free H<sub>2</sub>O. Extracellular vesicles were obtained by ultracentrifugation at  $110,000 \times g$  for 2 h at 4 °C, as previously described [30]. To ensure comparability, all fractions were used in the same concentrations as are present in PBMCsec. All fractions were tested separately and in a combined form. To reconstitute the fractions, equal volumes of each fraction were combined and further diluted to the equivalent concentration of PBMCsec.

### 2.4. Neutrophil Isolation

Neutrophils were isolated using the MACSxpress Whole Blood Neutrophil Isolation kit (Miltenyi Biotec, Bergisch-Gladbach, Germany) according to manufacturer's instructions. In brief, magnetic beads were resuspended in 2 mL of buffer A. One-fourth of the total amount of processed blood of magnetic beads and buffer B were added to the blood

and incubated at room temperature for 5 min under constant gentle rotation. Blood and isolation cocktail mix were placed in the MACSxpress Separator (Miltenyi Biotec) and allowed to separate for 15 min. Clear, neutrophil-containing top phase was transferred into a fresh tube and washed with basal RPMI 1640 without phenol red (Thermo Fisher Scientific, Waltham, USA). If required, a red blood cell lysis was performed using a Red Blood Cell Lysis Buffer (Abcam, Cambridge, UK) for 10 to 15 min at room temperature. Neutrophils were resuspended in basal RPMI 1640 in an assay dependent concentration without phenol red for further use.

### 2.5. Induction of NET Formation

Either isolated neutrophils or whole blood samples after red blood cell lysis were pre-treated with 2 units/mL PBMcsec or equivalent vehicle medium for 20 min at 37 °C. Cells were then stimulated with 5 µM ionomycin (Sigma Aldrich, St. Louis, MO, USA) or 100 nm phorbol 12-myristate 13-acetate (PMA) (Sigma Aldrich), or 10 µM Thapsigargin (Abcam) for 2 h at 37 °C unless indicated otherwise.

### 2.6. Flow Cytometry

After stimulation with indicated compounds, cells were centrifuged and stained with anti-citrullinated Histone H3 antibody (ab5103, Abcam) to detect NETs, anti-CD66b antibody (pacific-blue conjugated mouse anti-human, clone G10F5, BioLegend, San Diego, CA, USA) and anti-CD15 antibody (4hycoerythrin-cyanine 7 conjugated mouse anti-human, clone W6D3, BioLegend) to identify neutrophils. Flow cytometric analysis was performed using BD FACSCanto II and BD FACSDiva software (version 6.1.3) (BD Pharmingen, San Jose, CA, USA).

### 2.7. Cell Viability Assay

Incucyte Cytotox Dye for Counting Dead Cells (Sartorius, Goettingen, Germany) was used according to the manufacturer's instructions. In brief, cells were treated as indicated, followed by the addition of 250 nm cytotox green dye for staining 100 µL cell suspension in a concentration of  $4 \times 10^6$  cells/mL condition in a 96-well plate. Cell death was assessed over the indicated time periods in a microplate reader at an excitation wavelength of 485 nm and an emission wavelength of 520 nm. Microplate reader (BMG Labtech, FLUOstar OPTIMA) and the BMG Labtech Optima software (software version 2.20Rs, BMG Labtech, Ortenberg, Germany).

### 2.8. EZ4U Cell Proliferation and Cytotoxicity Assay

EZ4U (Biomedica, Vienna, Austria) assay was performed according to manufacturer's instructions. Briefly, the substrate was dissolved in 2.5 mL activator solution and pre-warmed to 37 °C. Then, a 20 µL substrate was added to 200 µL cell suspension at a concentration of  $4 \times 10^6$  cells per condition in a 96-well plate and incubated for 2 h. Continuous absorbance measurements at 450 nm were performed using a microplate reader (BMG Labtech, FLUOstar OPTIMA) and the BMG Labtech Optima software (software version 2.20Rs).

### 2.9. ROS Production Measurement

ROS production was measured using the DCFD/H2DCFDA cellular ROS assay kit (Abcam). Cells were treated as indicated and the assay was performed as recommended by the manufacturer.

### 2.10. $Ca^{2+}$ Flux Measurement

Ratiometric calcium flux measurements with Fura Red were performed as described by Wendt et al., with minor modifications [39]. In brief, a cell suspension of  $4 \times 10^6$  cells per condition, either isolated neutrophils or whole blood, pre-treated with PBMcsec or vehicle for 20 min as indicated, were washed, resuspended in 400 µL full medium containing 1 µM

Fura Red (Invitrogen, Thermo Fisher Scientific, Waltham, MA, USA), and incubated for 30 min at 37 °C. Cells were washed once with medium, resuspended in 4 mL medium and incubated for another 30 min at 37 °C. Subsequently, cells were rested on ice for up to 30 min. Data were acquired on a FACS Aria III flow cytometer (BD Bioscience, San Jose, CA, USA). Before intracellular calcium flux measurement, 1 mL of Fura Red-loaded cells was transferred to a FACS tube and pre-warmed for 5 min at 37 °C in a water bath. The cells were kept at 37 °C during the whole measurement. The baseline response was recorded for 30 s prior to stimulation with 5 µM ionomycin. Changes in calcium mobilization were recorded for a total of 120 s. Fura Red was excited using a 405 nm violet laser and a 561 nm green laser and changes in emission were detected with a 635 LP, 660/20 BP, and a 655 LP, 795/40 BP filter set, respectively. The 'Fura Red Ratio' over time was calculated using the Kinetics tool in FlowJo software (version 9.3.3, Tree Star Inc., Ashland, OR, USA) as follows:

$$\text{Fura Red Ratio} = \frac{\text{increase of 405 nm induced emission}}{\text{decrease of 561 nm induced emission}}$$

#### 2.11. DNase Activity Measurement

DNase activity was measured by incubating 0.25 µg/µL Lambda DNA with 0.5 M acetate/NaOH at pH 4.8 (Merck Millipore), 50 mM CaCl<sub>2</sub> (Merck Millipore), 50 mM MgCl<sub>2</sub> (Sigma-Aldrich, St. Louis, MO, USA), 40 mM 2-mercaptoethanol (Merck Millipore) and either 2 units/mL PBMCsec or equivalent vehicle control or DNase I (Thermo Fisher Scientific) as positive control for 1 h at 37 °C. 10 µL of each sample were loaded into a 1% agarose gel with gel red (Biotium, Fremont, CA, USA) together with 2 µL 6x loading dye (Thermo Fisher Scientific). Electrophoresis was performed at 200 V for 35 min. DNase activity was determined by absence of λ-DNA.

#### 2.12. Proteome Profiler

The Human Apoptosis Array kit (R&D Systems, Minneapolis, MN, USA) was used in accordance with the manufacturer's instructions with no modifications. Isolated neutrophils were treated as indicated and cell lysates of 4 × 10<sup>6</sup> cells per condition of 4 individual donors were pooled.

#### 2.13. PAD4 Inhibitor Assay

The inhibitory capacity of PBMCsec was measured using the PAD4 inhibitor Screening Assay kit (ammonia, Cayman Chemical, Ann Arbor, MI, USA) and performed according to manufacturer's instructions.

#### 2.14. Western Blot Analysis

For Western blot analysis, cells were lysed in 1x Laemmli sample Buffer (Bio-Rad Laboratories, CA, USA) supplemented with Protease Inhibitor Cocktail (Sigma-Aldrich). After sonication SDS-PAGE electrophoresis was performed on 4–20% gradient gels (Criterion TGX Precast Gels, Bio-Rad Laboratories). Proteins were electrotransferred onto 0.2 µM nitrocellulose membranes (Trans-Blot Turbo, Bio-Rad Laboratories) and immunodetected using primary antibodies against pan phospho-PKC (βII Ser660) antibody (#9371, Cell Signaling Technology, Danvers, MA, USA). This antibody detects endogenous PKC α, β I, β II, δ, ε, η and θ isoforms phosphorylated at carboxy-terminal residue homologous to serine 660 of PKC βII. Peroxidase-conjugated secondary antibody were detected with the SuperSignal West Dura Extended Duration Substrate (Thermo Scientific, Rockford, MA, USA), according to manufacturer's instructions. A Ponceau S solution (Sigma-Aldrich) staining served as equal loading control.

### 2.15. Statistics

Statistical analyses were performed using Prism 8.0.1 (Graph Pad Prism). Data were shown  $\pm$  standard deviation (SD). One-way ANOVA and Sidak's multiple comparisons test were performed and \*  $p < 0.0332$ , \*\*  $p < 0.0021$ , \*\*\*  $p < 0.0002$ , \*\*\*\*  $p < 0.0001$ .

## 3. Results

### 3.1. PBMCsec Inhibits NET Formation

Although immunomodulatory properties of PBMCsec have been well described in a variety of different cell types [30,34,40], a potential effect of PBMCsec on neutrophils has not yet been explored. To investigate whether PBMCsec interferes with experimentally induced NET formation, we pre-incubated human whole blood with 2 units/mL PBMCsec or an equivalent dose of vehicle prior to stimulation with 5  $\mu$ M ionomycin. Unstimulated or PBMCsec-treated samples showed few citH3-positive neutrophils, identified by CD15<sup>+</sup>CD66b<sup>+</sup>citH3<sup>+</sup> staining (Figure 1A, upper panel and Figure 1B,  $2.4 \pm 0.97\%$  and  $1.6 \pm 1.22\%$  positive cells, respectively, Figure S1A). The addition of ionomycin strongly induced NET formation, as demonstrated by a significant increase in citH3-positive cells ( $54.52 \pm 14.41\%$ ) after two hours of incubation (Figure 1A, bottom panel and Figure 1B). This effect was almost completely abolished by pre-incubation with PBMCsec before ionomycin treatment ( $3.9 \pm 1.28\%$  citH3-positive neutrophils). A dose titration of PBMCsec revealed that 2 U/mL was the lowest dose with NET inhibiting activity (Figure S1C). By contrast, vehicle treatment showed only a weak reduction in NET-formation ( $27.94 \pm 17.71\%$  citH3-positive neutrophils) (Figure 1A, bottom panel, and Figure 1B). As DNA is one of the major constituents of NETs [4], we analysed the amount of extracellular DNA in ionomycin-stimulated samples using cytotox green staining (Figure 1C). After two hours, only a weak cytotox green signal was detected in untreated, PBMCsec, or vehicle treated samples. Although stimulation with ionomycin resulted in a drastic increase in extracellular DNA (Figure 1C), the addition of PBMCsec almost completely inhibited the release of DNA after ionomycin stimulation. To exclude the possibility that the observed effect was due to a direct inhibitory effect of PBMCsec on ionomycin, we also used PMA (100 nM), another well-described inducer of NET formation. As shown in Figure 1D, PMA treatment of PBMCsec pre-incubated neutrophils led to a comparable inhibition of DNA release. Additionally, we evaluated the metabolic activity of ionomycin-activated neutrophils [41]. Ionomycin-activation resulted in a prominent decrease in metabolic activity which, in contrast to vehicle treatment, was completely abolished by the addition of PBMCsec (Figure S1B). Immunostaining of neutrophils for citH3 showed classical NET-structures after ionomycin treatment, which were completely absent in the presence of PBMCsec (Figure 1E). Taken together, these findings indicate that treatment of experimentally activated neutrophils with PBMCsec significantly reduces the formation of NETs.

### 3.2. A Synergistic Effect of Different Substance Classes Inhibits NET Formation

PBMCsec is composed of different substance classes, including free DNA, lipids, proteins, and extracellular vesicles [34,35,38,42] (Figure 2A). Thus, we further aimed to investigate to what extent the individual fractions contribute to the inhibitory effects on NET formation (Figure 2B,C). Therefore, PBMCsec and its fractions were added to whole blood prior to ionomycin stimulation and citH3 levels were analysed (Figures 2B,C and S2). Ionomycin treatment showed a significant increase in citH3<sup>+</sup> neutrophils, which was almost completely abolished by the addition of PBMCsec. In contrast, purified fractions showed only partial inhibition of ionomycin-induced histone citrullination, indicating that the inhibitory effect of PBMCsec requires the complex interplay of all fractions of the secretome. Stimulation with the reconstituted fractions of PBMCsec fully restores the inhibitory activity of NET formation (Figure 2B,C).

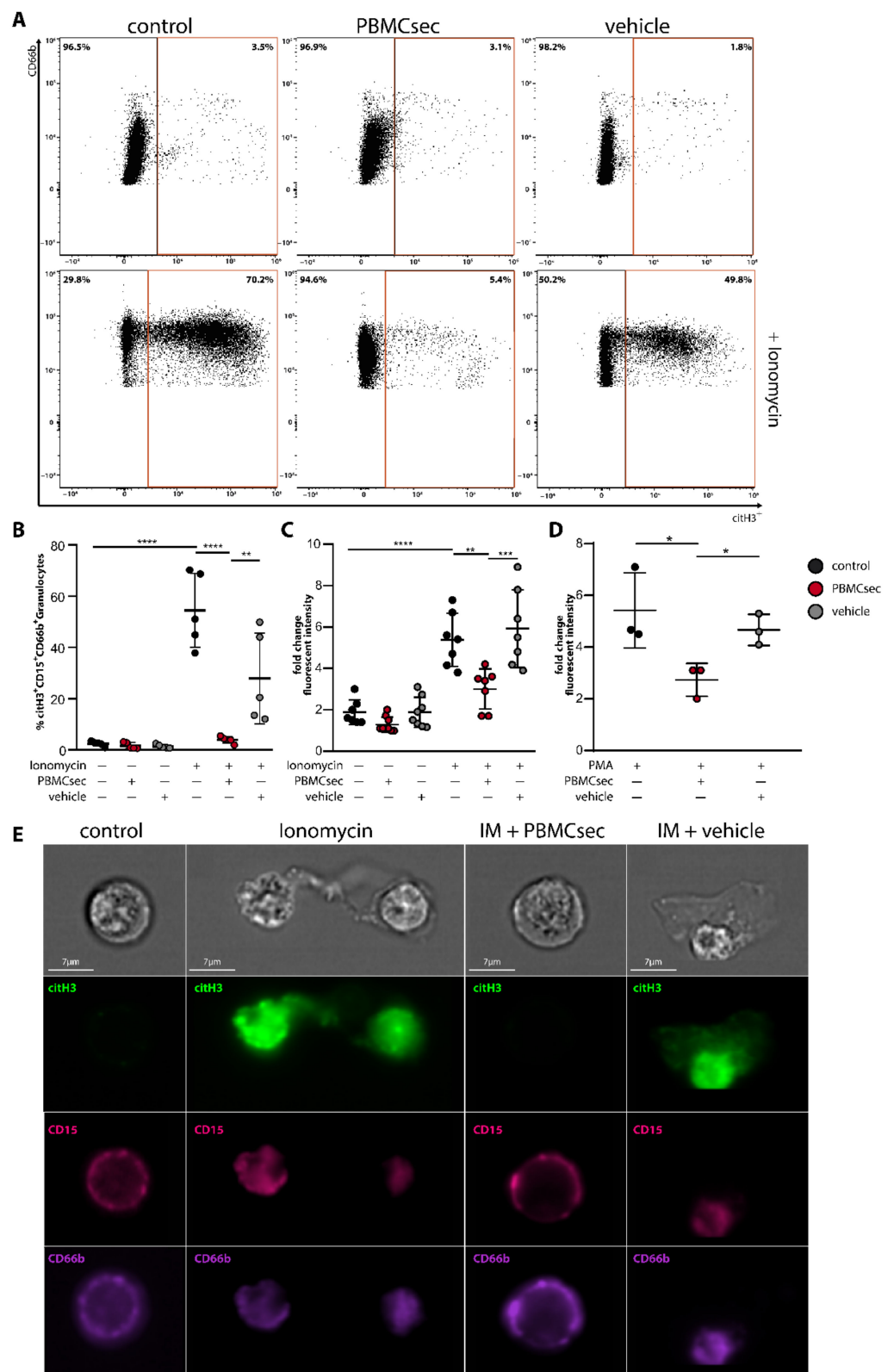


**Figure 1.** PBMCsec inhibits NET formation. Erythrocyte-lysed blood was treated with PBMCsec or vehicle for 20 min and subsequently stimulated with ionomycin (IM) for 2 h and analysed with flow cytometry, cytotox staining, and image stream analysis. (A) Neutrophils were identified in flow cytometry as CD66b<sup>+</sup>CD15<sup>+</sup> cells and NET-forming neutrophils were characterized by citH3. Control, PBMCsec, or vehicle treated samples are shown in the top panel and ionomycin-activated neutrophils are shown in the bottom panel. *n* = 5. One representative sample is shown out of five

replicates summarized in (B). (C) Extracellular DNA content was measured using cytotox staining of neutrophils after pre-treatment with PBMCsec or vehicle and subsequent activation for 2 h with (C) IM or (D) PMA. Fold change increase in relative fluorescent intensity is shown after two hours of stimulation relative to time point zero/start of stimulation/minute one after induction of NETs. (E) Visualization of IM-activated neutrophils was performed using image stream analyses. Untreated (control) and IM-PBMCsec treated neutrophils did not show citH3<sup>+</sup> staining. IM and IM-vehicle treated neutrophils showed robust citH3<sup>+</sup> staining of cells and additional extracellular structures (indicative for NETs). Green, citH3; magenta, CD15; purple, CD66b; *n* = 2. One representative sample is shown. Data are represented as individual values with mean and error bars indicate SD, one-way ANOVA and Sidak’s multiple comparisons test. \* *p* < 0.0332, \*\* *p* < 0.0021, \*\*\* *p* < 0.0002, \*\*\*\* *p* < 0.0001.

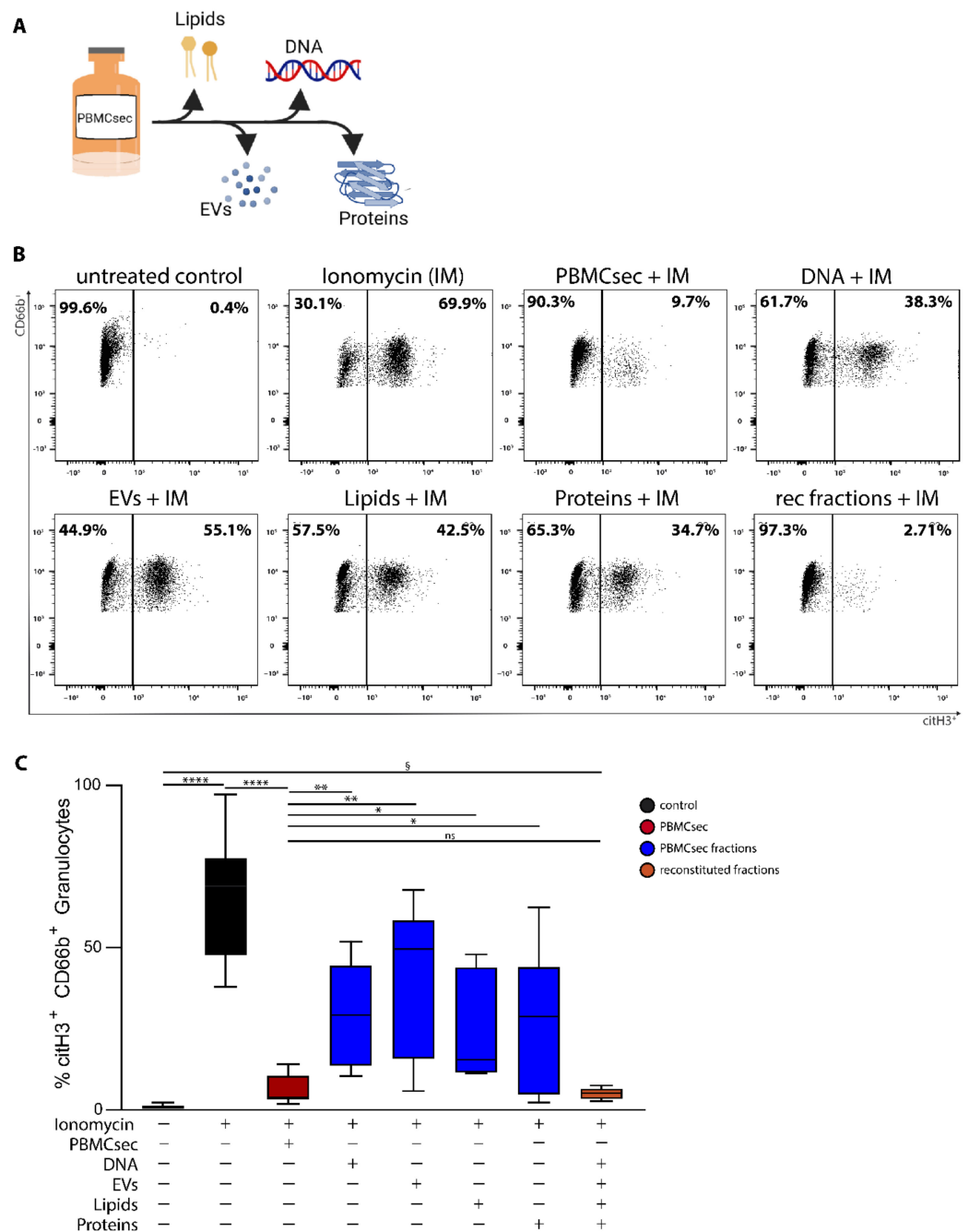


**Figure 2.** Isolated substance classes of PBMCsec show a synergistic effect on NET-inhibition. (A) Schematic depiction of the isolated and tested substance classes of PBMCsec. This scheme was

created with BioRender.com, accessed on 2 June 2022 (B) Neutrophils were identified in flow cytometry as CD66b<sup>+</sup>CD15<sup>+</sup> cells and NET formation was characterized by citH3<sup>+</sup> signal. rec fractions + IM = reconstituted fractions + ionomycin. n = 6. One representative sample out of six is shown, summarized in (C) one-way ANOVA and Sidak’s multiple comparisons test. Data are represented as mean and error bars indicate SD. § = ANOVA without multiple comparison tests,  $p < 0.0001$ ; \*  $p < 0.0332$ , \*\*  $p < 0.0021$ , \*\*\*\*  $p < 0.0001$ .

### 3.3. PBMCsec Does Not Show DNase-Activity

As digestion of NETs by DNases is the main NETs-clearing mechanism [43], we next investigated whether PBMCsec displays DNase activity. Therefore, we incubated λDNA with PBMCsec and analysed DNA degradation (Figure 3A). Compared to recombinant DNase I, which completely digested λDNA, PBMCsec showed no DNA degrading activity (Figure 3A). Since this in vitro assay was optimized for DNase I only, we further tested potential NETs-degrading properties of PBMCsec in whole blood ex vivo. For this purpose, we stimulated whole blood with ionomycin and applied PBMCsec either prior to or two hours after ionomycin treatment (Figure 3B). In contrast to neutrophils treated with PBMCsec prior to their activation, treatment two hours after induction of NET formation did not reduce the amount of citH3 positive neutrophils (Figure 3C,D and Figure S3). These data demonstrate that PBMCsec does not degrade pre-formed NETs by DNases, suggesting an active intervention in the NET-forming signalling cascade.

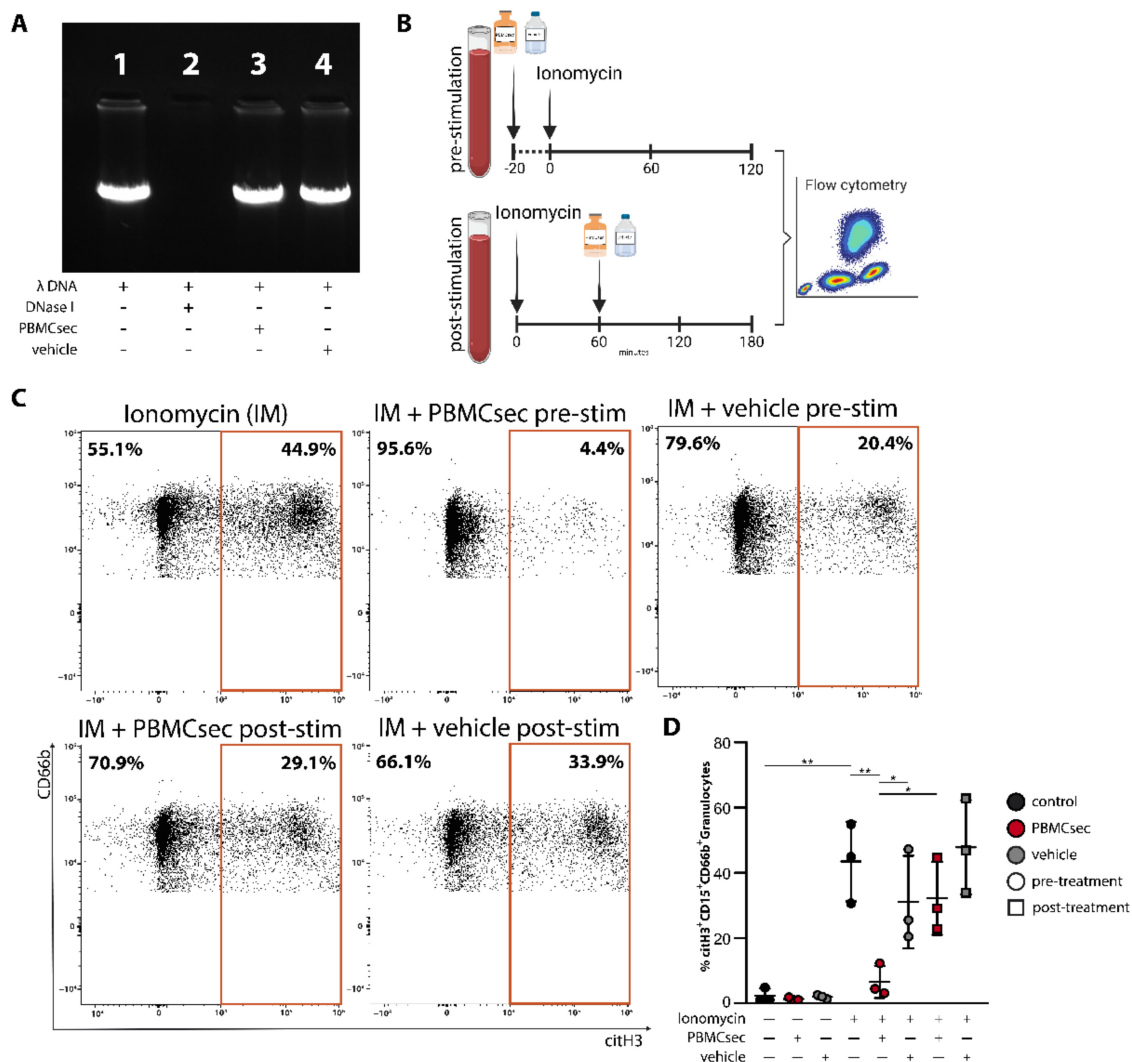
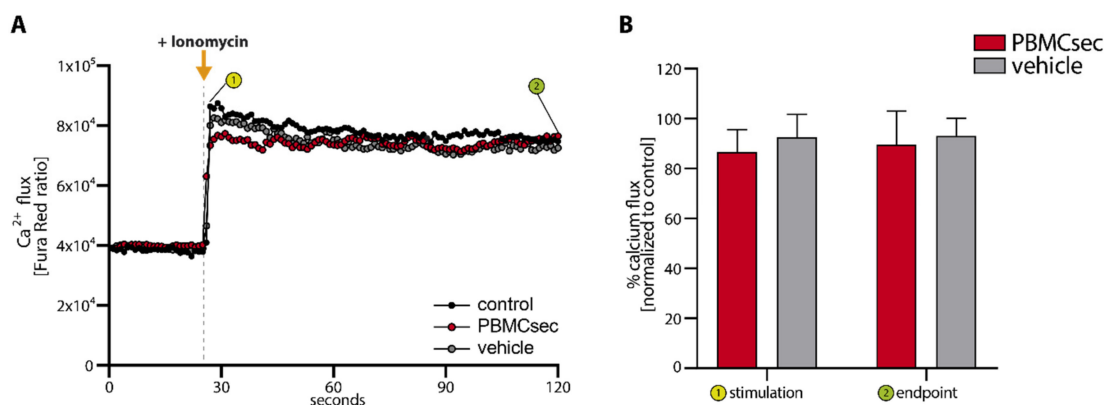


Figure 3. PBMCsec inhibits NET formation by a DNase-independent mode of action. (A) DNase

activity was measured in a cell-free assay by co-incubation of PBMcsec or vehicle with  $\lambda$ -DNA. DNase I was used as positive control.  $n = 3$ , one representative sample is shown. (B) Schematic depiction of the adapted neutrophil stimulation protocol for the measurement of potential DNase activity in a cell-based assay. This scheme was created with BioRender.com, accessed on 2 June 2022 (C) Neutrophils were identified as CD66b<sup>+</sup>CD15<sup>+</sup> cells and citH3<sup>+</sup> signal was used to characterize NET formation.  $n = 3$ , one representative experiment is shown. (D) Statistical summary of all biological donors is shown. Data are represented as individual values with mean and error bars indicate SD. One-way ANOVA and Sidak's multiple comparisons test. \*  $p < 0.0332$ , \*\*  $p < 0.0021$ .

### 3.4. PBMcsec Inhibits NET Formation by Preventing ROS Production and PAD4 Activity

Induction of NETs requires an increase in intracellular calcium levels [8,9,11]. We, therefore, first investigated whether PBMcsec interferes with ionomycin-induced calcium influx. Analysis of intracellular calcium signalling, using a Fura Red based flow cytometry approach, revealed that pre-treatment of whole blood with PBMcsec only marginally reduced calcium influx after addition of ionomycin (Figure 4A,B). The decline in calcium flux was only transient and returned to control values rapidly. No significant difference was observed between PBMcsec and vehicle treatment, suggesting that the observed decrease in the calcium influx is not sufficient to affect NET formation. In addition, we also tested Thapsigargin, an irreversible inhibitor of the sarco-endoplasmic reticulum Ca<sup>2+</sup>-ATPase (SERCA) pumps, which prevents the storage of excess intracellular calcium in the endoplasmic reticulum [44]. The addition of 10  $\mu$ M Thapsigargin induced NET formation comparably to ionomycin (Figure S4). Furthermore, PBMcsec was able to counteract Thapsigargin-induced NET formation (Figure S4) very efficiently. Together, these findings indicate that PBMcsec does not interfere with calcium flux in neutrophils and suggest that its NET-inhibiting action is mediated downstream of calcium flux. As increased intracellular calcium concentrations promote the activity of PKC [9], we next investigated PKC phosphorylation by Western blot analysis, using a pan phosphor-PKC antibody. As this antibody detects several phosphorylated isoforms of PKC, an assignment to a specific isoform was not possible. However, we were not able to detect differences in the amount of phosphorylated PKC after pre-treating neutrophils with PBMcsec or vehicle (data not shown), suggesting that the inhibitory action of PBMcsec is also downstream of PKC.



**Figure 4.** PBMcsec inhibits NET formation without interfering with calcium flux. (A) Ratiometric calcium flux was measured with Fura Red in neutrophils. Neutrophils were observed for approximately 30 s to record a baseline Fura Red ratio indicating homeostatic calcium flux prior to the addition of IM and subsequent analysis for a total of 120 s. (B) Statistical analysis of the percent reduction in calcium flux in PBMcsec or vehicle treated neutrophils compared to control samples is shown for the time points of stimulation (①, addition of IM) and the endpoint (②, 120 s)  $n = 4$ . Error bars indicate SD. No statistically significant reduction was observed for PBMcsec or vehicle treatment.

Since activation of the NET signalling pathway down-stream of NADPH leads to the production of ROS and activation of PAD4 [8,10,11], we next investigated whether PBMcsec

exerts its inhibitory activity by modulating these processes. We, therefore, investigated ionomycin-induced production of ROS using the cell permeant reagent 2',7'-dichlorofluorescein diacetate (DCFDA). Ionomycin treatment of PBMCsec-stimulated neutrophils resulted in a significant decrease in ROS production, as compared to ionomycin treatment alone (Figure 5A). By contrast, pre-treatment with vehicle showed no inhibitory effect (Figure 5A). Analysis of protein expression revealed that PBMCsec inhibited ionomycin-induced down-regulation of known anti-oxidative factors, including hemoxygenase-1 (HO-1) [45] and hypoxia inducible factor 1 alpha (HIF-1 $\alpha$ ) [46] in purified human neutrophils (Figures 5B and S5B), which was not observed in vehicle-treated cells.

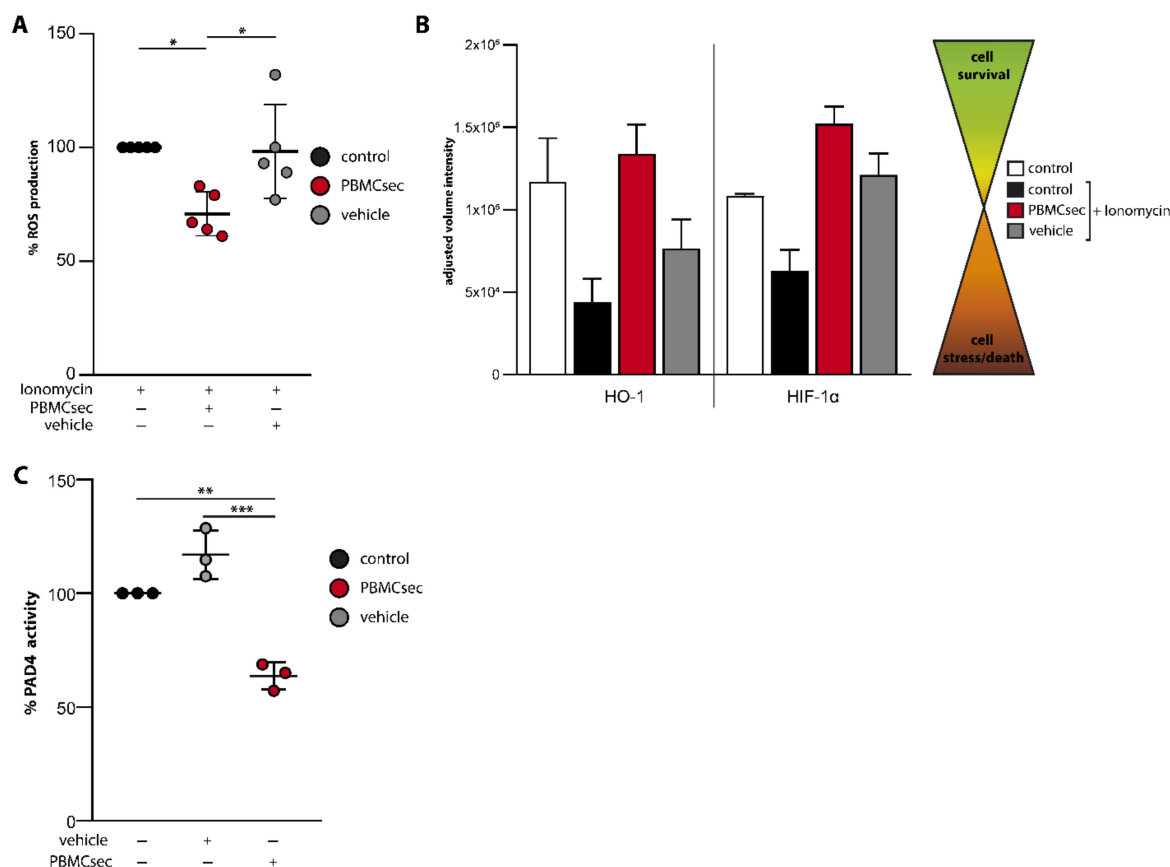


**Figure 5.** PBMCsec prevents ROS production and PAD4 activity. (A) ROS production in IM stimulated and PBMCsec or vehicle treated neutrophils normalized to IM-induced ROS production.  $n = 5$  (B) Analysis of protein levels of HO-1 and HIF-1 $\alpha$  of isolated neutrophils stimulated with ionomycin and treated with PBMCsec or vehicle, using a proteome profiler is shown. Cell lysates of four individual donors and experiments were pooled. Error bars indicate SD of two technical replicates. (C) Enzymatic activity of PAD4 was measured in a cell-free assay upon co-incubation of PBMCsec or vehicle with the PAD4-substrate and normalized to untreated control.  $n = 3$ , data are represented as individual values with mean and error bars indicate SD, unless indicated otherwise. One-way ANOVA and Sidak's multiple comparisons test was performed where significances are indicated. \*  $p < 0.0332$ , \*\*  $p < 0.0021$ , \*\*\*  $p < 0.0002$ .

The activation of PAD4 with subsequent histone-citrullination represents one of the final steps in the NETs signalling pathway [11]. Thus, we next investigated PAD4 activity in a cell-free assay. Although vehicle treatment did not show PAD4 inhibiting properties, PBMCsec inhibited PAD4 activity by approximately 40% (Figure 5C). Together, these data demonstrate that PBMCsec exerts its inhibitory activity on NET formation by reducing intracellular ROS production and preventing PAD4 activation.

#### 4. Discussion

The formation of NETs is a highly effective first line defence mechanism against invading pathogens [17]. However, there is growing evidence that excessive NETs formation contributes to tissue damage and the induction of auto-immune diseases [16,47–49]. Although several substances, including acetylsalicylic acid, cyclosporine A [50], metformin [51] and chloroquine [52], have been shown to influence NET formation, therapeutic drugs targeting NET formation are so far not available. In the current study, we provide evidence that PBM-Csec effectively inhibited NET formation by reducing ROS production and PAD4 activation, thereby providing a novel potential cell-derived but cell-free therapeutic intervention for NET-associated diseases.

The tissue regenerative and anti-inflammatory action spectrum of PBM-Csec is multifaceted [29,32,34,37,38,53,54], and most of its beneficial effects have been shown to require the interplay of several components of the secretome [30,55]. Indeed, we also found that NET formation was only fully inhibited when neutrophils were treated with the whole secretome or reconstituted purified fractions. Since we observed NETs inhibition at different steps of the NETs signalling pathway, we hypothesize that individual secretome fractions act on different signalling molecules. Recently, Laggner et al. showed that lipids present in PBM-Csec attenuate skin inflammation and allergic reactions by targeting dendritic cell function [34], as well as mast cell and basophil activation, respectively [56], suggesting that lipids are mainly responsible for the anti-inflammatory activities of PBM-Csec. Several lipid species have been detected in PBM-Csec, including phosphatidylserines, lysophosphatidylcholines, lysophosphatidylethanolamines, phosphatidylcholines, phosphatidylethanolamines, and resolvins [34]. Interestingly, several studies described a NET-inhibitory or NET-resolving action of resolvins [57–59]. Spinosa et al. demonstrated a decreased NET burden accompanied by reduced abdominal aortic aneurysm in reslovin-treated mice [57]. In addition, neutrophils derived from reslovin-treated mice showed less susceptibility to ionomycin-induced NET formation [58]. Although both of these studies identified less NET formation in the presence of resolvins, Chiang et al. showed that NETs formed after *Staphylococcus aureus* infection were more efficiently cleared by macrophages after treatment with reslovins [59]. These data indicate an important function of resolvins in the prevention of NET formation and/or resolution of NETs. Therefore, it is conceivable that the partial inhibition of NET formation observed by PBM-Csec-lipids may be explained by the variety of resolvins found in PBM-Csec [34]. However, whether PBM-Csec-derived resolvins or other lipid classes are indeed involved in PBM-Csec-induced NETs inhibition needs to be determined in future studies.

In addition to the lipid fraction, PBM-Csec-derived proteins also showed a strong inhibitory action on NET formation. Previous studies demonstrated that addition of either bovine or human serum albumin to ionomycin-treated cells almost completely blocked NET formation by chelating calcium [60]. However, as we only detected a slight decrease in calcium influx after treatment with PBM-Csec and vehicle, a sole albumin-dependent effect is unlikely. Additionally, PBM-Csec treatment also abrogated Thapsigargin-induced NETosis, which indicates that PBM-Csec-mediated NETosis inhibition occurs without interfering with calcium flux or the cells' capability to store excess calcium into intracellular storage units, such as the endoplasmic reticulum. Furthermore, we also showed comparable effects when NET formation was induced with PMA, which induces NETs in a calcium-independent manner. Together, our data suggest a calcium- and albumin-independent mode of action of the protein fraction of PBM-Csec. Further in-depth proteomics analyses of PBM-Csec-derived proteins are required to elucidate whether a single protein or a combination of proteins is responsible for the inhibition of NET formation.

Our data suggest the inhibition of ROS production and PAD4 activation as the two major modes of action for the reduction in NET formation by PBM-Csec. Oxidative stress, especially the generation of ROS, is a hallmark of NET formation [10,61] and HSPs are known to effectively block excessive ROS production [62]. Our study revealed that PBM-Csec inhibited hemeoxygenase 1 (HO-1 or HSP32) and HIF-1 $\alpha$  downregulation during

ionomycin-induced NET formation. Both HO-1 and HIF-1 $\alpha$  have been shown to promote neutrophil survival by reducing ROS levels [63] and via Akt and NF $\kappa$ B signalling under stress, respectively [46,64]. These data suggest that PBMsec contributes to the stabilization of the delicate balance of pro- and anti-oxidative processes by regulating the expression of HSPs, thereby preventing neutrophil-induced tissue damage. Since HO-1 is also known to downregulate adhesion molecules and chemokines required for neutrophil infiltration [45], PBMsec may alleviate inflammatory responses by reducing neutrophil infiltration in damaged and inflamed tissue. However, further studies are required to unravel the exact mechanism by which PBMsec counteracts ROS production as it is not yet clear whether it functions as ROS-scavenger, inhibits the liberation of ROS from mitochondria or if it interferes with the functional assembly of NADPH oxidase subunits.

PAD4 is one of the most prominently investigated factors critical for NET formation, and PAD inhibitors have been extensively studied in the context of a broad variety of diseases, including multiple sclerosis [65], myocardial infarction [66], and rheumatoid arthritis [67]. However, the exact mechanism of PAD4 inhibition is not yet fully understood [67]. Our data indicate that stressed PBMCs secrete factors that serve as PAD4 inhibitors. Interestingly, Yost et al. identified a group of peptides in umbilical cord blood with strong PAD4-inhibiting effects, leading to inhibition of NETs [68]. Sequence analyses identified  $\alpha$ 1-antitrypsin, a serine protease inhibitor, known to possess immunomodulatory and anti-inflammatory properties [69], as the main PAD4-inhibiting factor. Interestingly,  $\alpha$ 1-antitrypsin is synthesized by circulating monocytes and, therefore, a component of PBMsec (Figure S6) [70]. According to our quantification analysis, 25–30 ng/mL SERPINA1 are present in two units of PBMsec. This enzyme inhibitor has been considered as an acute phase protein, which contributes to the inhibition of NET formation by targeting a vast array of factors contributing to NET formation [71]. Further studies are needed to identify the PAD4-inhibiting factor(s) in PBMsec.

## 5. Conclusions

In summary, we have demonstrated a strong NETs-inhibitory activity of PBMsec via a dual mechanism. Specifically the identification of a PAD4 inhibitor, produced naturally in the human body, as well as the prevention of ROS production might strongly improve the treatment of diseases associated with excessive NET formation, such as rheumatoid arthritis [67], multiple sclerosis [65], sepsis [17], heart failure, and myocardial infarction [66]. Pre-clinical toxicological evaluation of PBMsec has already been performed without the occurrence of major adverse events after topical and intravenous application (LPT, study number 35015). Therefore, our study has paved the way for a clinical study in humans, assessing the potency of PBMsec in NETs-associated diseases in vivo.

**Supplementary Materials:** The following supporting information can be downloaded at: <https://www.mdpi.com/article/10.3390/antiox11081559/s1>, Graphical abstract: PBMsec inhibits NET formation; Figure S1: Gating strategy, PBMsec improves neutrophil metabolic activity; Figure S2: Flow cytometric analysis of spontaneous NET formation; Figure S3: Flow cytometric analysis of unstimulated neutrophils; Figure S4: PBMsec inhibits Thapsigargin-induced NETosis; Figure S5: Gating strategy and purity of isolated neutrophils; Figure S6: SERPINA1 abundance in PBMsec.

**Author Contributions:** Conceptualization, K.K., M.M., and H.J.A.; methodology, K.K., M.M., A.S.O., and T.M.H.; validation K.K., M.M., A.S.O., T.M.H.; formal analysis, K.K.; investigation, K.K., A.S.O., T.M.H., and K.P.; resources, H.J.A.; data curation, K.K., D.C., M.D., and D.B.; writing—original draft preparation, K.K. and M.M.; writing—review and editing, K.K., M.M., M.L., and A.M.; visualization, K.K.; supervision, M.M.; project administration, K.K. and M.M.; funding acquisition, H.J.A. All authors have read and agreed to the published version of the manuscript.

**Funding:** This research project was financed in part by the Austrian Research Promotion Agency grant “APOSEC” (852748 and 862068, 2015–2019), by the Vienna Business Agency “APOSEC to clinic,” (2343727, 2018–2020), and by the Aposcience AG under group leader H.J.A., M.M. was funded by Aposcience AG.

**Institutional Review Board Statement:** The study was conducted in accordance with the Declaration of Helsinki, and approved by the Institutional Ethical Review Board of the Medical University of Vienna (protocol code 1539/2017).

**Informed Consent Statement:** Informed consent was obtained from all subjects involved in the study.

**Data Availability Statement:** Data is contained within the article or Supplementary Materials.

**Acknowledgments:** We thank H.P. Haselsteiner and the CRISCAR Familienstiftung for their belief in this private–public partnership to augment basic and translational clinical research.

**Conflicts of Interest:** The Medical University of Vienna has claimed financial interest. H.J.A. holds patents related to this work (WO 2010/079086 A1; WO 2010/070105 A1).

## References

1. Rosales, C. Neutrophil: A cell with many roles in inflammation or several cell types? *Front. Physiol.* **2018**, *9*, 113.
2. Nicolás-Ávila, J.Á.; Adrover, J.M.; Hidalgo, A. Neutrophils in Homeostasis, Immunity, and Cancer. *Immunity* **2017**, *46*, 15–28. [[CrossRef](#)]
3. Brinkmann, V.; Zychlinsky, A. Beneficial suicide: Why neutrophils die to make NETs. *Nat. Rev. Microbiol.* **2007**, *5*, 577–582. [[CrossRef](#)] [[PubMed](#)]
4. Brinkmann, V.; Reichard, U.; Goosmann, C.; Fauler, B.; Uhlemann, Y.; Weiss, D.S.; Weinrauch, Y.; Zychlinsky, A. Neutrophil Extracellular Traps Kill Bacteria. *Science* **2004**, *303*, 1532–1535. [[CrossRef](#)] [[PubMed](#)]
5. Futosi, K.; Fodor, S.; Mócsai, A. Neutrophil cell surface receptors and their intracellular signal transduction pathways. *Int. Immunopharmacol.* **2013**, *17*, 638–650. [[CrossRef](#)] [[PubMed](#)]
6. Fuchs, T.A.; Abed, U.; Goosmann, C.; Hurwitz, R.; Schulze, I.; Wahn, V.; Weinrauch, Y.; Brinkmann, V.; Zychlinsky, A. Novel cell death program leads to neutrophil extracellular traps. *J. Cell Biol.* **2007**, *176*, 231–241. [[CrossRef](#)]
7. Kenny, E.F.; Herzig, A.; Krüger, R.; Muth, A.; Mondal, S.; Thompson, P.R.; Brinkmann, V.; von Bernuth, H.; Zychlinsky, A. Diverse stimuli engage different neutrophil extracellular trap pathways. *eLife* **2017**, *6*, e24437. [[CrossRef](#)]
8. Wang, Y.; Li, M.; Stadler, S.; Correll, S.; Li, P.; Wang, D.; Hayama, R.; Leonelli, L.; Han, H.; Grigoryev, S.A.; et al. Histone hypercitrullination mediates chromatin decondensation and neutrophil extracellular trap formation. *J. Cell Biol.* **2009**, *184*, 205–213. [[CrossRef](#)]
9. Kaplan, M.J.; Radic, M. Neutrophil Extracellular Traps: Double-Edged Swords of Innate Immunity. *J. Immunol.* **2012**, *189*, 2689–2695. [[CrossRef](#)]
10. Sollberger, G.; Tilley, D.O.; Zychlinsky, A. *Neutrophil Extracellular Traps: The Biology of Chromatin Externalization*; Cell Press: Cambridge, MA, USA, 2018; Volume 44, pp. 542–553.
11. Rohrbach, A.S.; Slade, D.J.; Thompson, P.R.; Mowen, K.A. Activation of PAD4 in NET formation. *Front. Immunol.* **2012**, *3*, 360. [[CrossRef](#)]
12. Papayannopoulos, V.; Metzler, K.D.; Hakkim, A.; Zychlinsky, A. Neutrophil elastase and myeloperoxidase regulate the formation of neutrophil extracellular traps. *J. Cell Biol.* **2010**, *191*, 677–691. [[CrossRef](#)]
13. Neeli, I.; Dwivedi, N.; Khan, S.; Radic, M. Regulation of extracellular chromatin release from neutrophils. *J. Innate Immun.* **2009**, *1*, 194–201. [[CrossRef](#)] [[PubMed](#)]
14. Kolaczowska, E.; Kubes, P. Neutrophil recruitment and function in health and inflammation. *Nat. Rev. Immunol.* **2013**, *13*, 159–175. [[CrossRef](#)]
15. Thålin, C.; Hisada, Y.; Lundström, S.; Mackman, N.; Wallén, H. Neutrophil Extracellular Traps. *Arterioscler. Thromb. Vasc. Biol.* **2019**, *39*, 1724–1738. [[CrossRef](#)]
16. Wang, J. Neutrophils in tissue injury and repair. *Cell Tissue Res.* **2018**, *371*, 531–539. [[CrossRef](#)]
17. Fine, N.; Tasevski, N.; McCulloch, C.A.; Tenenbaum, H.C.; Glogauer, M. The Neutrophil: Constant Defender and First Responder. *Front. Immunol.* **2020**, *11*, 571085. [[CrossRef](#)]
18. Wculek, S.K.; Malanchi, I. Neutrophils support lung colonization of metastasis-initiating breast cancer cells. *Nature* **2015**, *528*, 413–417. [[CrossRef](#)]
19. Gupta, A.K.; Joshi, M.B.; Philippova, M.; Erne, P.; Hasler, P.; Hahn, S.; Resink, T.J. Activated endothelial cells induce neutrophil extracellular traps and are susceptible to NETosis-mediated cell death. *FEBS Lett.* **2010**, *584*, 3193–3197. [[CrossRef](#)]
20. Mangold, A.; Ondracek, A.S.; Hofbauer, T.M.; Scherz, T.; Artner, T.; Panagiotides, N.; Beitzke, D.; Ruzicka, G.; Nistler, S.; Wohlschläger-Krenn, E.; et al. Culprit site extracellular DNA and microvascular obstruction in ST-elevation myocardial infarction. *Cardiovasc. Res.* **2021**, *118*, 2006–2017. [[CrossRef](#)]
21. Mangold, A.; Hofbauer, T.M.; Ondracek, A.S.; Artner, T.; Scherz, T.; Speidl, W.S.; Krychtiuk, K.A.; Sadushi-Kolici, R.; Jakowitsch, J.; Lang, I.M. Neutrophil extracellular traps and monocyte subsets at the culprit lesion site of myocardial infarction patients. *Sci. Rep.* **2019**, *9*, 16304. [[CrossRef](#)]
22. Distelmaier, K.; Winter, M.P.; Dragschitz, F.; Redwan, B.; Mangold, A.; Gleiss, A.; Perkmann, T.; Maurer, G.; Adlbrecht, C.; Lang, I.M. Prognostic value of culprit site neutrophils in acute coronary syndrome. *Eur. J. Clin. Investig.* **2014**, *44*, 257–265. [[CrossRef](#)] [[PubMed](#)]

23. Fadini, G.P.; Menegazzo, L.; Rigato, M.; Scattolini, V.; Poncina, N.; Bruttocao, A.; Ciciliot, S.; Mammano, F.; Ciubotaru, C.D.; Brocco, E.; et al. NETosis delays diabetic wound healing in mice and humans. *Diabetes* **2016**, *65*, 1061–1071. [[CrossRef](#)] [[PubMed](#)]
24. Kitching, A.R.; Anders, H.J.; Basu, N.; Brouwer, E.; Gordon, J.; Jayne, D.R.; Kullman, J.; Lyons, P.A.; Merkel, P.A.; Savage, C.O.S.; et al. ANCA-associated vasculitis. *Nat Rev Dis Prim.* **2020**, *6*, 71. [[CrossRef](#)] [[PubMed](#)]
25. Meegan, J.E.; Yang, X.; Beard, R.S.; Jannaway, M.; Chatterjee, V.; Taylor-Clark, T.E.; Yuan, S.Y. Citrullinated histone 3 causes endothelial barrier dysfunction. *Biochem. Biophys. Res. Commun.* **2018**, *503*, 1498–1502. [[CrossRef](#)] [[PubMed](#)]
26. Klopff, J.; Brostjan, C.; Eilenberg, W.; Neumayer, C. Neutrophil extracellular traps and their implications in cardiovascular and inflammatory disease. *Int. J. Mol. Sci.* **2021**, *22*, 559. [[CrossRef](#)]
27. Natallya, F.; Herwanto, N.; Prakoeswa, C.; Indramaya, D.; Rantam, F. Effective healing of leprosy chronic plantar ulcers by application of human amniotic membrane stem cell secretome gel. *Indian J. Dermatol.* **2019**, *64*, 250. [[CrossRef](#)] [[PubMed](#)]
28. Karpov, A.A.; Puzanov, M.V.; Ivkin, D.Y.; Krasnova, M.V.; Anikin, N.A.; Docshin, P.M.; Moiseeva, O.M.; Galagudza, M.M. Non-inferiority of microencapsulated mesenchymal stem cells to free cells in cardiac repair after myocardial infarction: A rationale for using paracrine factor(s) instead of cells. *Int. J. Exp. Pathol.* **2019**, *100*, 102–113. [[CrossRef](#)] [[PubMed](#)]
29. Ankersmit, H.J.; Hoetzenecker, K.; Dietl, W.; Soleiman, A.; Horvat, R.; Wolfsberger, M.; Gerner, C.; Hacker, S.; Mildner, M.; Moser, B.; et al. Irradiated cultured apoptotic peripheral blood mononuclear cells regenerate infarcted myocardium. *Eur. J. Clin. Investig.* **2009**, *39*, 445–456. [[CrossRef](#)] [[PubMed](#)]
30. Wagner, T.; Traxler, D.; Simader, E.; Beer, L.; Narzt, M.S.; Gruber, F.; Madlener, S.; Laggner, M.; Erb, M.; Vorstandlechner, V.; et al. Different pro-angiogenic potential of  $\gamma$ -irradiated PBMC-derived secretome and its subfractions. *Sci. Rep.* **2018**, *8*, 18016. [[CrossRef](#)]
31. Mildner, C.S.; Copic, D.; Zimmermann, M.; Lichtenauer, M.; Direder, M.; Klas, K.; Bormann, D.; Gugerell, A.; Moser, B.; Hoetzenecker, K.; et al. Secretome of Stressed Peripheral Blood Mononuclear Cells Alters Transcriptome Signature in Heart, Liver, and Spleen after an Experimental Acute Myocardial Infarction: An In Silico Analysis. *Biology* **2022**, *11*, 116. [[CrossRef](#)] [[PubMed](#)]
32. Beer, L.; Zimmermann, M.; Mitterbauer, A.; Ellinger, A.; Gruber, F.; Narzt, M.S.; Zellner, M.; Gyöngyösi, M.; Madlener, S.; Simader, E.; et al. Analysis of the secretome of apoptotic peripheral blood mononuclear cells: Impact of released proteins and exosomes for tissue regeneration. *Sci. Rep.* **2015**, *5*, 16662. [[CrossRef](#)]
33. Kasiri, M.M.; Beer, L.; Nemeč, L.; Gruber, F.; Pietkiewicz, S.; Haider, T.; Simader, E.M.; Traxler, D.; Schweiger, T.; Janik, S.; et al. Dying blood mononuclear cell secretome exerts antimicrobial activity. *Eur. J. Clin. Investig.* **2016**, *46*, 853–863. [[CrossRef](#)] [[PubMed](#)]
34. Laggner, M.; Copic, D.; Nemeč, L.; Vorstandlechner, V.; Gugerell, A.; Gruber, F.; Peterbauer, A.; Ankersmit, H.J.; Mildner, M. Therapeutic potential of lipids obtained from  $\gamma$ -irradiated PBMCs in dendritic cell-mediated skin inflammation: PBMC lipid secretome and DC functions. *eBioMedicine* **2020**, *55*, 102774. [[CrossRef](#)] [[PubMed](#)]
35. Beer, L.; Mildner, M.; Gyöngyösi, M.; Ankersmit, H.J. Peripheral blood mononuclear cell secretome for tissue repair. *Apoptosis* **2016**, *21*, 1336–1353. [[CrossRef](#)] [[PubMed](#)]
36. Pavo, N.; Zimmermann, M.; Pils, D.; Mildner, M.; Petrás, Z.; Petneházy, Ö.; Fuzik, J.; Jakab, A.; Gabriel, C.; Sipos, W.; et al. Long-acting beneficial effect of percutaneously intramyocardially delivered secretome of apoptotic peripheral blood cells on porcine chronic ischemic left ventricular dysfunction. *Biomaterials* **2014**, *35*, 3541–3550. [[CrossRef](#)]
37. Panahipour, L.; Kargarpour, Z.; Laggner, M.; Mildner, M.; Ankersmit, H.J.; Gruber, R. TGF- $\beta$  in the Secretome of Irradiated Peripheral Blood Mononuclear Cells Supports In Vitro Osteoclastogenesis. *Int. J. Mol. Sci.* **2020**, *21*, 8569. [[CrossRef](#)]
38. Panahipour, L.; Kochergina, E.; Laggner, M.; Zimmermann, M.; Mildner, M.; Ankersmit, H.J.; Gruber, R. Role for lipids secreted by irradiated peripheral blood mononuclear cells in inflammatory resolution in vitro. *Int. J. Mol. Sci.* **2020**, *21*, 4694. [[CrossRef](#)]
39. Wendt, E.R.; Ferry, H.; Greaves, D.R.; Keshav, S. Ratiometric Analysis of Fura Red by Flow Cytometry: A Technique for Monitoring Intracellular Calcium Flux in Primary Cell Subsets. *PLoS ONE* **2015**, *10*, e0119532. [[CrossRef](#)]
40. Hacker, S.; Mittermayr, R.; Nickl, S.; Haider, T.; Leberherz-Eichinger, D.; Beer, L.; Mitterbauer, A.; Leiss, H.; Zimmermann, M.; Schweiger, T.; et al. Paracrine Factors from Irradiated Peripheral Blood Mononuclear Cells Improve Skin Regeneration and Angiogenesis in a Porcine Burn Model. *Sci. Rep.* **2016**, *6*, 25168. [[CrossRef](#)]
41. Schimek, V.; Strasser, K.; Beer, A.; Göber, S.; Walterskirchen, N.; Brostjan, C.; Müller, C.; Bachleitner-Hofmann, T.; Bergmann, M.; Dolznig, H.; et al. Tumour cell apoptosis modulates the colorectal cancer immune microenvironment via interleukin-8-dependent neutrophil recruitment. *Cell Death Dis.* **2022**, *13*, 113. [[CrossRef](#)]
42. Simader, E.; Traxler, D.; Kasiri, M.M.; Hofbauer, H.; Wolzt, M.; Glogner, C.; Storka, A.; Mildner, M.; Gouya, G.; Geusau, A.; et al. Safety and tolerability of topically administered autologous, apoptotic PBMC secretome (APOSEC) in dermal wounds: A randomized Phase 1 trial (MARSYAS I). *Sci. Rep.* **2017**, *7*, 6216. [[CrossRef](#)] [[PubMed](#)]
43. Jiménez-Alcázar, M.; Rangaswamy, C.; Panda, R.; Bitterling, J.; Simsek, Y.J.; Long, A.T.; Bilyy, R.; Krenn, V.; Renné, C.; Renné, T.; et al. Host DNases prevent vascular occlusion by neutrophil extracellular traps. *Science* **2017**, *358*, 1202–1206. [[CrossRef](#)] [[PubMed](#)]
44. Ribeiro, D.; Freitas, M.; Rocha, S.; Lima, J.L.F.C.; Carvalho, F.; Fernandes, E. Calcium Pathways in Human Neutrophils—The Extended Effects of Thapsigargin and ML-9. *Cells* **2018**, *7*, 204. [[CrossRef](#)] [[PubMed](#)]
45. Seldon, M.P.; Silva, G.; Pejanovic, N.; Larsen, R.; Gregoire, I.P.; Filipe, J.; Anrather, J.; Soares, M.P. Heme oxygenase-1 inhibits the expression of adhesion molecules associated with endothelial cell activation via inhibition of NF- $\kappa$ B RelA phosphorylation at serine 276. *J. Immunol.* **2007**, *179*, 7840–7851. [[CrossRef](#)] [[PubMed](#)]

46. Zhang, Z.; Yao, L.; Yang, J.; Wang, Z.; Du, G. PI3K/Akt and HIF-1 signaling pathway in hypoxia-ischemia (Review). *Mol. Med. Rep.* **2018**, *18*, 3547–3554. [[CrossRef](#)] [[PubMed](#)]
47. Villanueva, E.; Yalavarthi, S.; Berthier, C.C.; Hodgin, J.B.; Khandpur, R.; Lin, A.M.; Rubin, C.J.; Zhao, W.; Olsen, S.H.; Klinker, M.; et al. Netting Neutrophils Induce Endothelial Damage, Infiltrate Tissues, and Expose Immunostimulatory Molecules in Systemic Lupus Erythematosus. *J. Immunol.* **2011**, *187*, 538–552. [[CrossRef](#)] [[PubMed](#)]
48. Boufenzar, A.; Carrasco, K.; Jolly, L.; Brustolin, B.; Di-Pillo, E.; Derive, M.; Gibot, S. Potentiation of NETs release is novel characteristic of TREM-1 activation and the pharmacological inhibition of TREM-1 could prevent from the deleterious consequences of NETs release in sepsis. *Cell. Mol. Immunol.* **2021**, *18*, 452–460. [[CrossRef](#)] [[PubMed](#)]
49. Barnado, A.; Crofford, L.J.; Oates, J.C. At the Bedside: Neutrophil extracellular traps (NETs) as targets for biomarkers and therapies in autoimmune diseases. *J. Leukoc. Biol.* **2016**, *99*, 265–278. [[CrossRef](#)]
50. Gupta, A.K.; Giaglis, S.; Hasler, P.; Hahn, S. Efficient Neutrophil Extracellular Trap Induction Requires Mobilization of Both Intracellular and Extracellular Calcium Pools and Is Modulated by Cyclosporine A. *PLoS ONE* **2014**, *9*, e97088.
51. Menegazzo, L.; Scattolini, V.; Cappellari, R.; Bonora, B.M.; Albiero, M.; Bortolozzi, M.; Romanato, F.; Ceolotto, G.; Vigili de Kreutzeberg, S.; Avogaro, A.; et al. The antidiabetic drug metformin blunts NETosis in vitro and reduces circulating NETosis biomarkers in vivo. *Acta Diabetol.* **2018**, *55*, 593–601. [[CrossRef](#)]
52. Boone, B.A.; Murthy, P.; Miller-Ocuin, J.; Doerfler, W.R.; Ellis, J.T.; Liang, X.; Ross, M.A.; Wallace, C.T.; Sperry, J.L.; Lotze, M.T.; et al. Chloroquine reduces hypercoagulability in pancreatic cancer through inhibition of neutrophil extracellular traps. *BMC Cancer* **2018**, *18*, 678. [[CrossRef](#)]
53. Hoetzenecker, K.; Zimmermann, M.; Hoetzenecker, W.; Schweiger, T.; Kollmann, D.; Mildner, M.; Hegedus, B.; Mitterbauer, A.; Hacker, S.; Birner, P.; et al. Mononuclear cell secretome protects from experimental autoimmune myocarditis. *Eur. Heart J.* **2015**, *36*, 676–685a. [[CrossRef](#)] [[PubMed](#)]
54. Lichtenauer, M.; Mildner, M.; Baumgartner, A.; Hasun, M.; Werba, G.; Beer, L.; Altmann, P.; Roth, G.; Gyöngyösi, M.; Podesser, B.K.; et al. Intravenous and intramyocardial injection of apoptotic white blood cell suspensions prevents ventricular remodelling by increasing elastin expression in cardiac scar tissue after myocardial infarction. *Basic Res. Cardiol.* **2011**, *106*, 645–655. [[CrossRef](#)] [[PubMed](#)]
55. Simader, E.; Beer, L.; Laggner, M.; Vorstandlechner, V.; Gugerell, A.; Erb, M.; Kalinina, P.; Copic, D.; Moser, D.; Spittler, A.; et al. Tissue-regenerative potential of the secretome of  $\gamma$ -irradiated peripheral blood mononuclear cells is mediated via TNFRSF1B-induced necroptosis. *Cell Death Dis.* **2019**, *10*, 729. [[CrossRef](#)] [[PubMed](#)]
56. Laggner, M.; Acosta, G.S.; Kitzmüller, C.; Copic, D.; Gruber, F.; Altenburger, L.M.; Vorstandlechner, V.; Gugerell, A.; Direder, M.; Klas, K.; et al. The secretome of irradiated peripheral blood mononuclear cells attenuates activation of mast cells and basophils. *eBioMedicine* **2022**, *81*, 104093. [[CrossRef](#)] [[PubMed](#)]
57. Spinosa, M.; Su, G.; Salmon, M.D.; Lu, G.; Cullen, J.M.; Fashandi, A.Z.; Hawkins, R.B.; Montgomery, W.; Meher, A.K.; Conte, M.S.; et al. Resolvin D1 Decreases Abdominal Aortic Aneurysm Formation by Inhibiting NETosis in a Mouse Model. *J. Vasc. Surg.* **2018**, *68*, 93S. [[CrossRef](#)]
58. Cherpokova, D.; Jouvène, C.C.; Libreros, S.; DeRoo, E.P.; Chu, L.; de La Rosa, X.; Norris, P.C.; Wagner, D.D.; Serhan, C.N. Resolvin D4 attenuates the severity of pathological thrombosis in mice. *Blood* **2019**, *134*, 1458–1468. [[CrossRef](#)]
59. Chiang, N.; Sakuma, M.; Rodriguez, A.R.; Spur, B.W.; Irimia, D.; Serhan, C.N. Resolvin T-series Reduce Neutrophil Extracellular Traps. *Blood* **2021**, *139*, 1222–1233. [[CrossRef](#)] [[PubMed](#)]
60. Neubert, E.; Senger-Sander, S.N.; Manzke, V.S.; Busse, J.; Polo, E.; Scheidmann, S.E.F.; Schön, M.P.; Kruss, S.; Erpenbeck, L. Serum and serum albumin inhibit in vitro formation of Neutrophil Extracellular Traps (NETs). *Front. Immunol.* **2019**, *10*, 12. [[CrossRef](#)] [[PubMed](#)]
61. Hakkim, A.; Fuchs, T.A.; Martinez, N.E.; Hess, S.; Prinz, H.; Zychlinsky, A.; Waldmann, H. Activation of the Raf-MEK-ERK pathway is required for neutrophil extracellular trap formation. *Nat. Chem. Biol.* **2011**, *7*, 75–77. [[CrossRef](#)] [[PubMed](#)]
62. Ikwegbue, P.C.; Masamba, P.; Oyinloye, B.E.; Kappo, A.P. Roles of heat shock proteins in apoptosis, oxidative stress, human inflammatory diseases, and cancer. *Pharmaceuticals* **2018**, *11*, 2. [[CrossRef](#)]
63. Li, X.; Schwacha, M.G.; Chaudry, I.H.; Choudhry, M.A. Heme Oxygenase-1 Protects against Neutrophil-Mediated Intestinal Damage by Down-Regulation of Neutrophil p47 phox and p67 phox Activity and O<sub>2</sub><sup>-</sup> Production in a Two-Hit Model of Alcohol Intoxication and Burn Injury. *J. Immunol.* **2008**, *180*, 6933–6940. [[CrossRef](#)] [[PubMed](#)]
64. Walmsley, S.R.; Print, C.; Farahi, N.; Peyssonnaud, C.; Johnson, R.S.; Cramer, T.; Sobolewski, A.; Condliffe, A.M.; Cowburn, A.S.; Johnson, N.; et al. Hypoxia-induced neutrophil survival is mediated by HIF-1 $\alpha$ -dependent NF- $\kappa$ B activity. *J. Exp. Med.* **2005**, *201*, 105–115. [[CrossRef](#)]
65. Sarswat, A.; Wasilewski, E.; Chakka, S.K.; Bello, A.M.; Caprariello, A.V.; Muthuramu, C.M.; Stys, P.K.; Dunn, S.E.; Kotra, L.P. Inhibitors of protein arginine deiminases and their efficacy in animal models of multiple sclerosis. *Bioorgan. Med. Chem.* **2017**, *25*, 2643–2656. [[CrossRef](#)] [[PubMed](#)]
66. Du, M.; Yang, W.; Schmul, S.; Gu, J.; Xue, S. Inhibition of peptidyl arginine deiminase-4 protects against myocardial infarction induced cardiac dysfunction. *Int. Immunopharmacol.* **2020**, *78*, 106055. [[CrossRef](#)]
67. Jones, J.E.; Causey, C.P.; Knuckley, B.; Slack-Noyes, J.L.; Thompson, P.R. Protein arginine deiminase 4 (PAD4): Current understanding and future therapeutic potential. *Curr. Opin. Drug Discov. Dev.* **2009**, *12*, 616–627.

68. Yost, C.C.; Schwertz, H.; Cody, M.J.; Wallace, J.A.; Campbell, R.A.; Vieira-De-Abreu, A.; Araujo, C.V.; Schubert, S.; Harris, E.S.; Rowley, J.W.; et al. Neonatal NET-inhibitory factor and related peptides inhibit neutrophil extracellular trap formation. *J. Clin. Investig.* **2016**, *126*, 3783–3798. [[CrossRef](#)]
69. Janciauskiene, S.M.; Bals, R.; Koczulla, R.; Vogelmeier, C.; Köhnlein, T.; Welte, T. The discovery of  $\alpha$ 1-antitrypsin and its role in health and disease. *Respir. Med.* **2011**, *105*, 1129–1139. [[CrossRef](#)]
70. Van Furth, R.; Kramps, J.A.; Diesselhof Den Dulk, M.M.C. Synthesis of  $\alpha$ 1-anti-trypsin by human monocytes. *Clin. Exp. Immunol.* **1983**, *51*, 551–557.
71. Janciauskiene, S.; Wrenger, S.; Immenschuh, S.; Olejnicka, B.; Greulich, T.; Welte, T.; Chorostowska-Wynimko, J. The multifaceted effects of Alpha1-Antitrypsin on neutrophil functions. *Front. Pharmacol.* **2018**, *9*, 341. [[CrossRef](#)] [[PubMed](#)]